

# Monte Carlo Simulation in InAs<sub>x</sub>P<sub>1-x</sub>, InAs and InP at High Field Application

<sup>1</sup>F. Nofeli and <sup>2</sup>M. Abedzadeh Fayzabadi

<sup>1</sup>Physics Department, Khayyam Higher Education University, Mashhad, Iran

<sup>2</sup>Physics Department, Payame Noor University, Fariman, Iran

## Abstract

We study how electrons, initially in thermal equilibrium, drift under the action of an applied electric field within bulk zincblende InAs<sub>x</sub>P<sub>1-x</sub>, InAs and InP. Calculations are made using a non-parabolic effective mass energy band model, Monte Carlo simulation that includes all of the major scattering mechanisms. The band parameters used in the simulation are extracted from optimized pseudopotential band calculations to ensure excellent agreement with experimental information and ab-initio band models. The effects of alloy scattering on the electron transport physics are examined. For all materials, it is found that electron velocity overshoot only occurs when the electric field is increased to a value above a certain critical field, unique to each material. This critical field is strongly dependent on the material parameters.

**Key words:** Non-parabolic; pseudopotential; alloy scattering; velocity overshoot.

## I. Introduction

InP and InAs offer the prospect of mobilities comparable to GaAs and are increasingly being developed for the construction of optical switches and optoelectronic devices. While GaAs has been extensively studied [1-3], InAs and InP and alloy constructed from them like InAs<sub>x</sub>P<sub>1-x</sub>, have yet to be examined to the same extent. Alloys of InAs and InP have unfortunately proved to be a difficult material to work with in practice and very little experimental work on InAs<sub>x</sub>P<sub>1-x</sub> material and devices has been done because of technical problems in forming Schottky contacts with sufficiently high barrier potentials. Nevertheless some experimental work has been done on other types of InAs and InP field-effect transistor, most notably MISFETs [4-5], and there is every reason to be optimistic that some form of heterojunction under the gate may well overcome the problem of the low barrier.

Improved electron transport properties are one of the main targets in the ongoing study of binary

and ternary InP, InAs and InAs<sub>x</sub>P<sub>1-x</sub> materials. The Monte Carlo technique has proved valuable for studying non-equilibrium carrier transport in a range of semiconductor materials and devices [6-7]. However, carrier transport modeling of InP and InAs materials has only recently begun to receive sustained attention, now that the growth of compounds and alloys is able to produce valuable material for the electronics industry. In this communication we present Monte Carlo calculations of steady-state and transient electron transport conditions in InP, InAs and InAs<sub>x</sub>P<sub>1-x</sub>. We demonstrate the effect of injection energy and electric field on the transient electron transport. The differences in transport properties are analyzed in terms of important material parameters. Our current approach employs a one-dimensional ensemble Monte Carlo technique to investigate

steady-state and transient electron transport in InP, InAs and InAs<sub>x</sub>P<sub>1-x</sub>. However, the momentum space treatment is three dimensional, and the scattering events consider all three dimensions. Specifically, our model includes the three lowest valleys of the conduction band with non-parabolicity.

## II. Model details

Our ensemble Monte Carlo simulations of electron transport in zincblende InP, InAs and InAs<sub>x</sub>P<sub>1-x</sub> are similar to those of Arabshahi et al [8-9]. As indicated earlier, a three-valley model for the conduction band is employed.

In order to calculate the electron drift velocity for large electric fields, consideration of conduction band satellite valleys is necessary. The first-principles band structure of zincblende InAs, InP and InAs<sub>x</sub>P<sub>1-x</sub> predicts a direct band gap located at the  $\Gamma$  point and lowest energy conduction band satellite valleys at the X point and at the L point. In our Monte Carlo simulation, the  $\Gamma$  valley, the three equivalent X valleys, the four equivalent L valleys, are represented by ellipsoidal, nonparabolic dispersion relationships. We assume that all donors are ionized and that the free-electron concentration is equal to the dopant concentration. For each simulation, the motion of ten thousand electron particles are examined, the temperature being set to 300 K, and the doping concentration being set to  $10^{17} \text{ cm}^{-3}$ . In the case of the ellipsoidal, non-parabolic conduction valley model, the usual Herring-Vogt transformation matrices are used to map carrier momenta into spherical valleys when particles are drifted or scattered. Electrons in bulk material suffer intravalley scattering by polar optical, non-polar optical and acoustic phonons scattering, intervalley phonons, and ionised impurity scattering. Acoustic scattering is assumed elastic and the absorption and emission rates are combined under the equipartition approximation, which is valid for lattice temperatures above 77 K. Elastic ionised impurity scattering is described using the screened Coulomb potential of the Brooks-Herring model.

## III. Results

Figure 1 shows the simulated velocity-field characteristics of zincblende InAs, InP, InAs<sub>0.2</sub>P<sub>0.8</sub> and InAs<sub>0.8</sub>P<sub>0.2</sub> semiconductors at 300 K, with a background doping concentration of  $10^{17} \text{ cm}^{-3}$ , and with the electric field applied along one of the cubic axes. The simulations suggest that the peak drift velocity for zincblende InAs is  $3.4 \times 10^5 \text{ ms}^{-1}$ , while that for InP, InAs<sub>0.2</sub>P<sub>0.8</sub> and InAs<sub>0.8</sub>P<sub>0.2</sub> are about  $\sim 2.3 \times 10^5 \text{ ms}^{-1}$ ,  $2.5 \times 10^5 \text{ ms}^{-1}$  and  $3.2 \times 10^5 \text{ ms}^{-1}$ , respectively. At higher electric fields, intervalley optical phonon emission dominates, causing the drift velocity to saturate at around  $1.5 \times 10^5 \text{ ms}^{-1}$  for all materials.

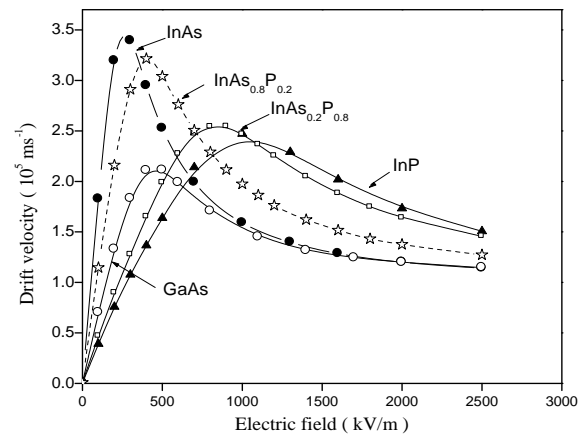


Figure 1: Calculated steady-state electron drift velocity in bulk zincblende InAs, InP, InAs<sub>0.2</sub>P<sub>0.8</sub> and InAs<sub>0.8</sub>P<sub>0.2</sub> using non-parabolic band models at room temperature.

The calculated drift velocities apparent from figure 1 are fractionally lower than those that have been calculated by Adachi et al. [14-16], who assumed an effective mass in the upper valleys equal to the free electron mass. The threshold field for the onset of significant scattering into satellite conduction band valleys is a function of the intervalley separation and the density of electronic states in the satellite valleys.

The valley occupancies for the  $\Gamma$ , X and L valleys are illustrated in figure 2 and show that the inclusion of

the satellite valleys in the simulation is important. Significant intervalley scattering into the satellite valleys occurs for fields above the threshold field for each material. This is important because electrons which are near a valley minimum have small kinetic energies and are therefore strongly scattered. It is apparent that intervalley transfer is substantially larger in InAs over the range of applied electric fields shown, due to the combined effect of a lower  $\Gamma$  effective mass, lower satellite valley separation energy, and slightly lower phonon scattering rate within the  $\Gamma$  valley.

We have also examined transient electron transport in bulk InAs, InP, InAs<sub>0.2</sub>P<sub>0.8</sub> and InAs<sub>0.8</sub>P<sub>0.2</sub> semiconductors. The transient response of electrons in these materials are compared in figure 3 for fields up to 1600 kV/m strengths. In InAs, we find very little or no overshoot occurs below the threshold field of 400 kV/m. As the electric field strength is increased to a value above the threshold field, overshoot begins to occur. As the field strength is increased further, both the peak overshoot velocity increases and the time for overshoot relaxation decreases.

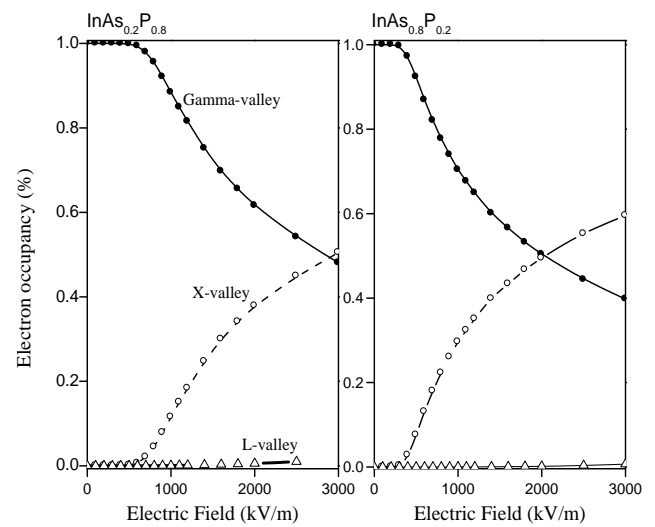
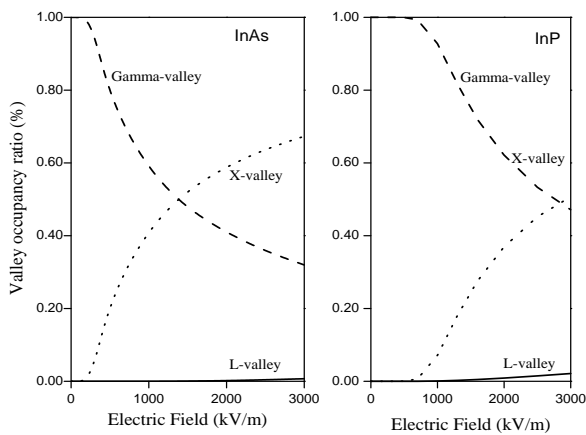
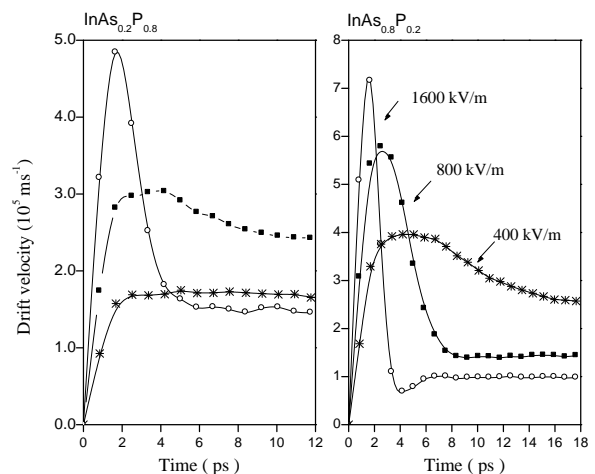


Figure 2: Fractional occupation of the central  $\Gamma$  and satellite valleys of zincblende InAs, InP, InAs<sub>0.2</sub>P<sub>0.8</sub> and InAs<sub>0.8</sub>P<sub>0.2</sub> as a function of applied electric field using the non-parabolic band model at room temperature.

In InAs, the velocity overshoot initially increases more rapidly with increasing electric field due to the lower  $\Gamma$  valley effective mass. For example, at 1600 kV/m, the maximum overshoot velocity for InAs is about  $8 \times 10^5$  ms<sup>-1</sup>, whereas for InP, InAs<sub>0.2</sub>P<sub>0.8</sub> and InAs<sub>0.8</sub>P<sub>0.2</sub> it is about  $4 \times 10^5$  ms<sup>-1</sup>,  $5 \times 10^5$  ms<sup>-1</sup> and  $7 \times 10^5$  ms<sup>-1</sup>, respectively. It is found also that for the same value of the electric field above the threshold value, the electron drift velocity is always smaller in InP, InAs<sub>0.2</sub>P<sub>0.8</sub> and InAs<sub>0.8</sub>P<sub>0.2</sub> than in InAs.



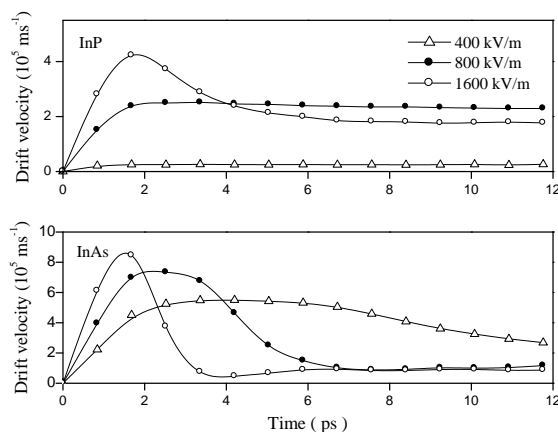


Figure 3: A comparison of the velocity overshoot effect exhibited by InAs, InP, InAs<sub>0.2</sub>P<sub>0.8</sub> and InAs<sub>0.8</sub>P<sub>0.2</sub> semiconductors as calculated by our Monte Carlo simulation. The donor concentration is 10<sup>17</sup> cm<sup>-3</sup> and the temperature is 300 K.

#### IV. Conclusions

Electron transport at 300 K in bulk zincblende InAs, InP, InAs<sub>0.2</sub>P<sub>0.8</sub> and InAs<sub>0.8</sub>P<sub>0.2</sub> have been simulated using an ensemble Monte Carlo simulation. Using valley models to describe the electronic bandstructure, calculated velocity-field characteristics are in fair agreement with other calculations. The velocity-field characteristics of the materials show similar trends, reflecting the fact that all the semiconductors have satellite valley effective densities of states several times greater than the central  $\Gamma$  valley.

#### References

[1] K. Brennan, K. Hess, J. Y. Tang and G. J. Iafrate, *IEEE Trans. Electron Devices*, **30**, 1750 (1983)  
 [2] N. Newman, T. Kendelewicz, L. Bowman and W. E. Spicer, *Appl. Phys. Lett.*, **46**, 1176 (1985)  
 [3] N. Newman, V. Schilfgaarde, T. Kendelewicz and W. E. Spicer, *Mater. Res. Soc. Symp. Proc.*, **54**, 443 (1986)  
 [4] D. C. Cameron, L. D. Irving, C. R. Whitehouse, *Thin Solid Films*, **103**, 61

(1983)  
 [5] D. C. Cameron, L. D. Irving, C. R. Whitehouse, *Electron. Lett.*, **18**, 534 (1982)  
 [6] C. Moglestue, *Monte Carlo Simulation of Semiconductor Devices*, 1993, Chapman and Hall  
 [7] C. Jacoboni and P. Lugli, *The Monte Carlo Method for semiconductor and Device Simulation*, 1989, Springer-Verlag  
 [8] H. Arabshahi, M. R. Benam and B. Salahi, *Modern Physics Letters B.*, **21**, 1715 (2007)  
 [9] H. Arabshahi, *Modern Physics Letters B.*, **21**, 199 (2007)  
 [10] B. E. Foutz, L. F. Eastman, U. V. Bhapkar and M. Shur, *Appl. Phys. Lett.*, **70**, 2849 (1997)  
 [11] U. V. Bhapkar and M. S. Shur, *J. Appl. Phys.*, **82**, 1649 (1997)  
 [12] J. D. Albrecht, R. P. Wang and P. P. Ruden, K F Brennan, *J. Appl. Phys.* **83**, 2185 (1998)  
 [13] E. O. Kane, *J. Phys. Chem. Solids*, **1**, 249 (1957)  
 [14] S. Adachi, *GaAs and Related Materials, Bulk semiconducting and Superlattice*